

How Müller Glial Cells in Macaque Fovea Coat and Isolate the Synaptic Terminals of Cone Photoreceptors

CHRISTINE BURRIS,¹ KARL KLUG,¹ IVY TRAN NGO,¹ PETER STERLING,²
AND STAN SCHEIN^{1,3*}

¹Department of Psychology, Franz Hall, University of California, Los Angeles,
Los Angeles, California, 90095-1563

²Department of Neuroscience, University of Pennsylvania, Philadelphia,
Pennsylvania, 19104

³Brain Research Institute, UCLA, Los Angeles, California, 90095-1761

ABSTRACT

A cone synaptic terminal in macaque fovea releases quanta of glutamate from ~20 active zones at a high rate in the dark. The transmitter reaches ~500 receptor clusters on bipolar and horizontal cell processes by diffusion laterally along the terminal's 50 μm^2 secretory face and ~2 μm inward. To understand what shapes transmitter flow, we investigated from electron photomicrographs of serial sections the relationship between Müller glial processes and cone terminals. We find that each Müller cell has one substantial trunk that ascends in the outer plexiform layer below the space between the "footprints" of the terminals. We find exactly equal numbers of Müller cell trunks and foveal cone terminals, which may make the fovea particularly vulnerable to Müller cell dysfunction. The processes that emerge from the single trunk do not ensheath a single terminal. Instead, each Müller cell partially coats two to three terminals; in turn, each terminal is completely coated by two to three Müller cells. Therefore, the Müller cells that coat one terminal also partially coat the surrounding (~ six) terminals, creating a common environment for the cones supplying the center/surround receptive field of foveal midget bipolar and ganglion cells. Upon reaching the terminals, the trunk divides into processes that coat the terminals' sides but not their secretory faces. This glial framework minimizes glutamate transporter (EAAT1) beneath a terminal's secretory face but maximizes EAAT1 between adjacent terminals, thus permitting glutamate to diffuse locally along the secretory face and inward toward inner receptor clusters but reducing its effective spillover to neighboring terminals. *J. Comp. Neurol.* 453:100–111, 2002.

© 2002 Wiley-Liss, Inc.

Indexing terms: cones (retina); fovea centralis; glia; neuroglia

The synaptic terminals of vertebrate photoreceptors release the neurotransmitter glutamate at a high tonic rate in the dark. To support this release rate, the cone terminal houses ~20 active zones, each served by a synaptic ribbon with a reservoir of ~100 tethered, synaptic vesicles. In the retina and elsewhere, when a synaptic vesicle releases its transmitter, the concentration in the synaptic cleft rises quickly and then decays in time and space (Clements, 1996; Rao-Mirotnik et al., 1998; Bergles et al., 1999). The details of this decay are important, because postsynaptic receptors near a release site, 10 nm across the synaptic cleft, would see high concentrations for a short time and ought to have low affinity and fast unbinding, whereas receptors farther from a release site would see lower concentrations for longer times and ought to have high affin-

ity and slow unbinding (Rao-Mirotnik et al., 1998; DeVries, 2000).

Geometry is critical because glia may physically isolate one synapse from another within a single terminal or the

Grant sponsor: UCLA Academic Senate; Grant number: EY11153; Grant number: EY08124.

*Correspondence to: Stan Schein, Department of Psychology, Franz Hall, Mailcode 951563, University of California, Los Angeles, Los Angeles, CA 90095-1563. E-mail: schein@ucla.edu

Received 11 February 2002; Revised 14 May 2002; Accepted 12 July 2002
DOI 10.1002/cne.10397

Published online the week of September 16, 2002 in Wiley InterScience (www.interscience.wiley.com).

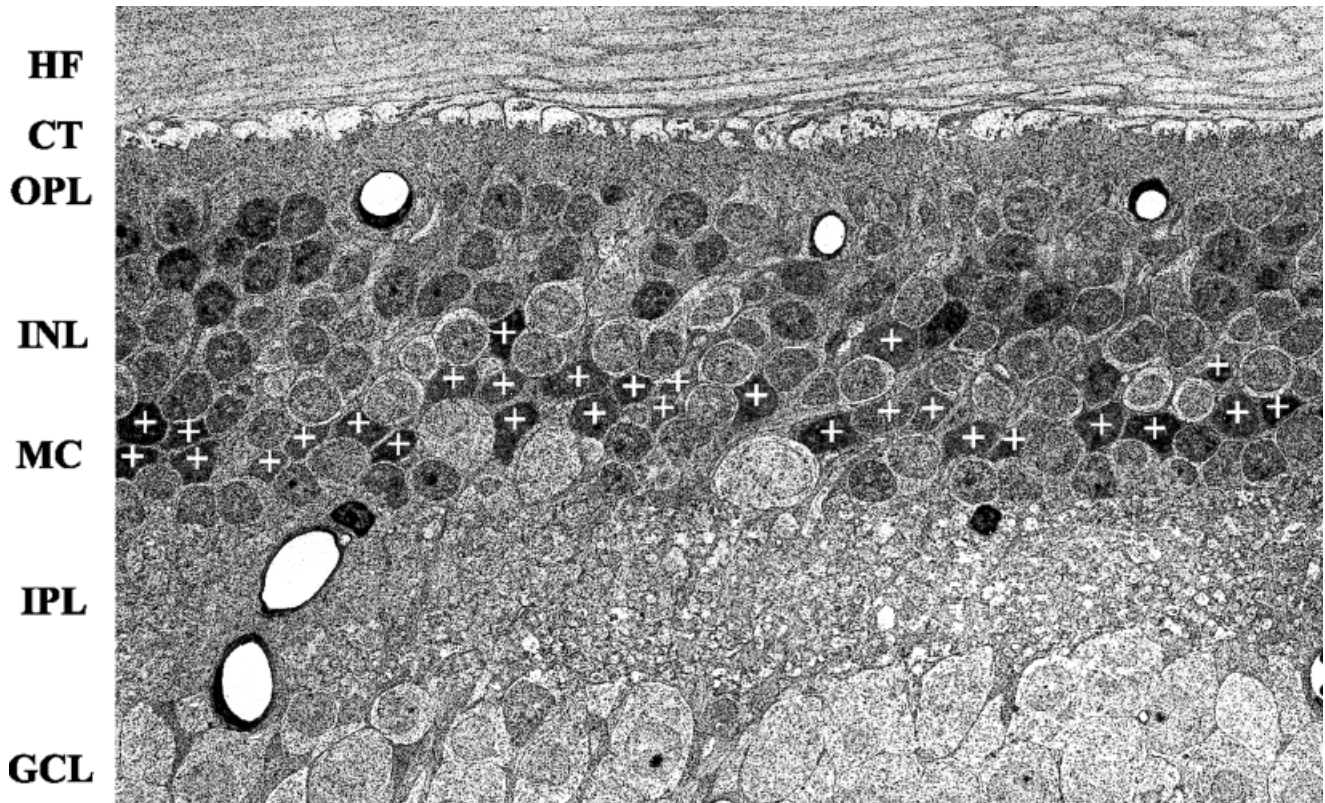


Fig. 1. Müller cell (MC) somas (+), typically polygonal in cross-section, are present with approximately the same incidence as the overlying cone terminals (CT). Vertical section through the macaque monkey retina centered at $560\ \mu\text{m}$ along the horizontal meridian,

connected to nasal foveal receptors at ~ 1 degree eccentricity (Tsukamoto et al., 1992). HF, Henle fibers; OPL, outer plexiform layer; INL, inner nuclear layer; IPL, inner plexiform layer; GCL, ganglion cell layer. Scale bar = $50\ \mu\text{m}$.

synapses of one terminal from those of another. In the cerebellum (Lehre and Danbolt, 1998), a single Bergman glial cell wraps the entire dendritic tree of a single Purkinje cell and coats every synapse (Ramón y Cajal, 1892; Spacek, 1985). By contrast, many glial processes wrap a hippocampal pyramidal cell and leave certain synapses naked (Ventura and Harris, 1999). Numerical relationships and glial-synaptic geometries are therefore specific for each brain region.

Such relationships have yet to be clarified in primate retina at the elaborate synaptic terminal of the cone photoreceptors, which is enveloped by glia called Müller cells (Müller, 1851; Ramón y Cajal, 1892; Dogiel, 1893). There, a quantal pulse of glutamate from the cone terminal diffuses $1\text{--}2\ \mu\text{m}$ both laterally and inward to ~ 500 sites where horizontal and bipolar cell dendrites express clusters of glutamate receptors (e.g., Schein et al., 1996; Herr et al., 1997; DeVries and Schwartz, 1999; DeVries, 2000; Haverkamp et al., 2000, 2001). The many pulses spread and merge to form a veritable river of glutamate whose flow ought to be primarily in the inward dimension from the secretory face into the outer synaptic layer. Here, we show that there is one Müller glial cell for each foveal cone terminal and describe quantitatively how Müller cells coat and isolate cone terminals, thus promoting flow primarily in the one dimension.

MATERIALS AND METHODS

This investigation used the same set of serial thin sections of the foveal retina of an adult male monkey (*Macaca fascicularis*) as was used in Tsukamoto et al. (1992), which gives details of preparation for electron microscopy. A series of 319 consecutive thin sections ($90\ \text{nm}$ thick) was cut vertically through the nasal fovea, parallel to the horizontal meridian, at a region connected to foveal cone outer segments at ~ 1 degree eccentricity (Tsukamoto et al., 1992). Sections were stained with uranyl acetate and lead citrate. The region spanning $480\ \mu\text{m}$ to $640\ \mu\text{m}$ from the foveal center was photographed at $400\times$, $2,000\times$, $5,000\times$, and $10,000\times$. From electron photomicrographs like the one shown in Figure 1, we determined the X (horizontal) and Y (vertical) coordinates of the center of each cone terminal. Electron photomicrographic negatives and positive prints were scanned with an Agfa scanner, and the tiff files were adjusted for brightness and contrast with Adobe Photoshop 5.0. No retouching or other image manipulation was performed.

The center points were plotted from $400\times$ photomicrographs onto clear plastic sheets and digitized by using the Montage software package (Smith, 1987). The schematic in Figure 2A shows how the terminals would appear in horizontal section. The Z coordinate of each center point

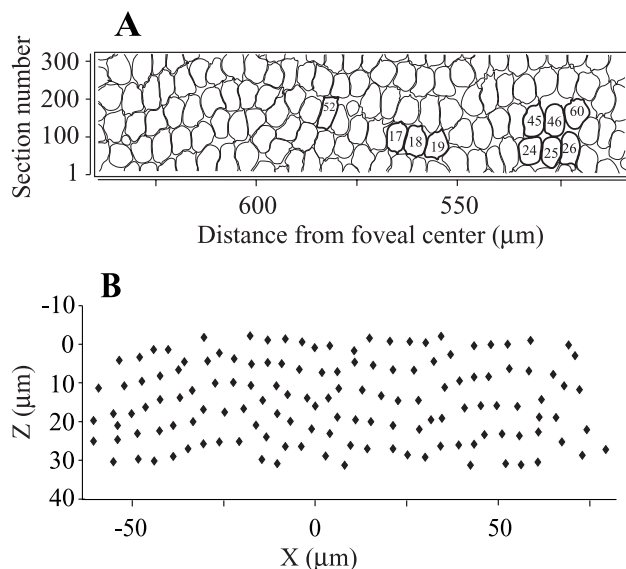


Fig. 2. Maps of the cone terminals in the horizontal plane. **A:** Schematic map of cone terminals, modified from Figure 5 of Tsukamoto et al. (1992); the numbered ones are those whose Müller cell coatings are quantified in Figures 6 and 7. **B:** Quantitative map of cone terminal centers corrected for vertical tilt during sectioning; X,Y coordinates of the cone terminal centers were obtained from the photomicrographs; Z coordinates were calculated as $28.71 \mu\text{m}$ minus the product of each terminal's center section number (from 1 to 319) and section thickness ($0.09 \mu\text{m}$).

was calculated as $28.71 \mu\text{m}$ minus the product of the number of the middle section and section thickness ($0.09 \mu\text{m}$). (The $28.71 \mu\text{m}$ derives from $319 \text{ sections} \times 0.09 \mu\text{m}$ per section.) For each terminal center, the X and Y coordinates were obtained from the photomicrograph of the middle section, not from the schematic, and projected onto the horizontal (XZ) plane (Fig. 2B).

Müller cell somas (Fig. 1) were electron dense and polygonal in shape. Most were located between the amacrine cell and bipolar cell somas. The coordinates of the Müller cell somas (taken as the center of their nuclei) in the inner nuclear layer and the coordinates of their trunks (see Results section) in the outer plexiform layer (OPL) were obtained by the same method.

The tissue had been cut slightly off the vertical; in addition, the photomicrographs were taken without demanding that the line of cone terminals, which establish the true horizontal, be horizontal in the photomicrographs. Consequently, we rotated the monolayer of terminals into the horizontal plane as follows: To correct for the angle off vertical, we best fit a line to the points projected into the YZ plane, computed the angle of that line, and rotated the cloud of points (about the X axis) by the opposite angle. Then, to correct for the angle off horizontal, we best fit a line to the new points projected into the XY plane, computed the angle of that line, and rotated the cloud of points (about the Z axis) by the opposite angle. The same cone-terminal-based rotations were applied to the coordinates of Müller cell somas and of Müller cell trunks.

RESULTS

Identical spatial densities of Müller cells and cone terminals

To compare the spatial densities of Müller cells and cone terminals, we first counted Müller cell nuclei and cone terminals. However, this method is only approximate because in the fovea Müller cell nuclei are displaced laterally from the cone terminals, which can cause large errors in calculating spatial densities (Schein, 1988). Also, we found that the array of outer midgrid bipolar nuclei did not replicate the array of cone terminals, so the mapping of Müller cell nuclei to their trunks in the outer retina may be similarly disorderly.

By tracing processes of 12 Müller cells at the level of the cone terminals, we found that each Müller soma emits a single trunk that ascends through the OPL (Fig. 3; also see Polyak, 1941; Robinson and Dreher, 1990; Dreher et al., 1992; Reichenbach et al., 1995). These trunks provide a good marker of each Müller cell at the same level as the cone terminals. Because the cone terminals and the Müller cell trunks are in the same layer, they could be mapped and counted in the same physical space.

We first determined the largest box that fully sampled the point patterns representing the centers of cone terminals (Fig. 4A) and Müller cell trunks (Fig. 4B). This box enclosed 101 cone terminals and 100 Müller cell trunks, suggesting that their densities are very similar. However, this method of analysis depends somewhat on the size of the box and its precise placement.

For greater accuracy, we counted the numbers of points representing either cone terminals or Müller cell trunks in boxes of increasing area. Then, plotting number of points vs. box size, we computed the best fitting line through the origin (Fig. 4C,D). This method smoothed the variation in measured density that arises from the discontinuous entry of points into expanding boxes. When box area increased beyond the larger box in Figure 4B, whose area was $3,813 \mu\text{m}^2$, the counts fell below the line in Figure 4D, indicating the limit of the area in which we had fully sampled Müller cell trunks. We therefore fit the points in Figure 4C,D up to the area of that box. The slopes of these lines are the densities: $26,961 \text{ terminals mm}^{-2}$ and $26,959 \text{ trunks mm}^{-2}$. The densities of terminals and trunks thus appear to be identical.

To further show that the similarity of the densities was not due to choice of the size of the largest box, we also graphed the number of trunks vs. the number of terminals contained in each counting box (Fig. 4E,F). With increasing area, the boxes first contain more terminals than trunks, then more trunks than terminals, and so forth. The best fitting line (Fig. 4F), however, had a slope of 0.999, confirming that the densities are the same.

As noted above, the density of Müller cells at the level of their nuclei gives only an approximate measure of the density of Müller cells at the level of the cone terminals. Nonetheless, we applied the same expanding box method as used for the Müller cell trunks (Fig. 4D) to the Müller cell nuclei and obtained a density of $27,163 \text{ mm}^{-2}$ ($r^2 = 0.989$), essentially equal to that of the Müller cell trunks and cone terminals.

How Müller cells coat the cone terminals

If each Müller cell completely ensheathed one cone terminal, the space between adjacent terminals would al-

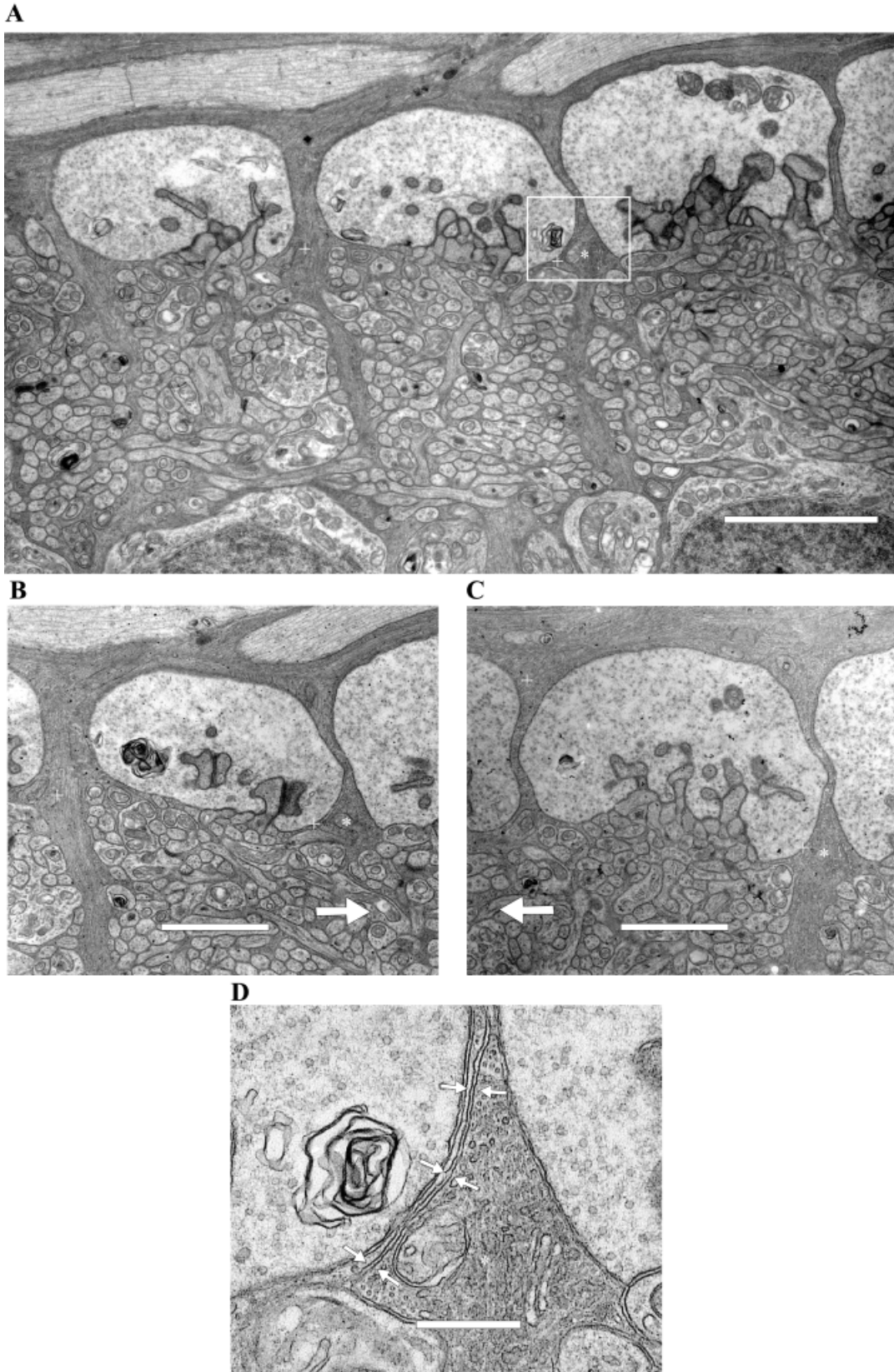


Fig. 3. Each Müller cell emits a single trunk that ascends through the neuropil below the region where cone terminals abut; upon reaching the terminals, it avoids their secretory faces. **A:** Vertical section through three cone terminals. The center terminal is flanked on the left by one Müller cell trunk (+) and on the right by a second trunk (*). The + trunk coats the right side of the left-hand terminal exclusively and the middle terminal on its left side and top. This + trunk then descends to coat the right side of the center terminal and is met by the ascending * trunk of the neighboring Müller cell (boxed region shown at higher magnification in D). **B:** Full thickness of the left Müller cell

trunk (+) is captured three sections forward from A. The right Müller cell trunk (*) has disappeared, replaced by neuropil, so transmitter may diffuse in the direction of the arrow to the neuropil underneath the adjacent cone terminal. **C:** Full thickness of the right Müller cell trunk (*) is captured six sections back from A. The left Müller cell trunk (+) has disappeared, replaced by neuropil, so transmitter may diffuse in the direction of the arrow. **D:** Boxed region from A at higher magnification. The arrows point to the membranes between the two (+ and *) Müller cell trunks that isolate the middle and right terminals, respectively. Scale bars = 3 μm in A, 2 μm in B,C, 0.5 μm in D.

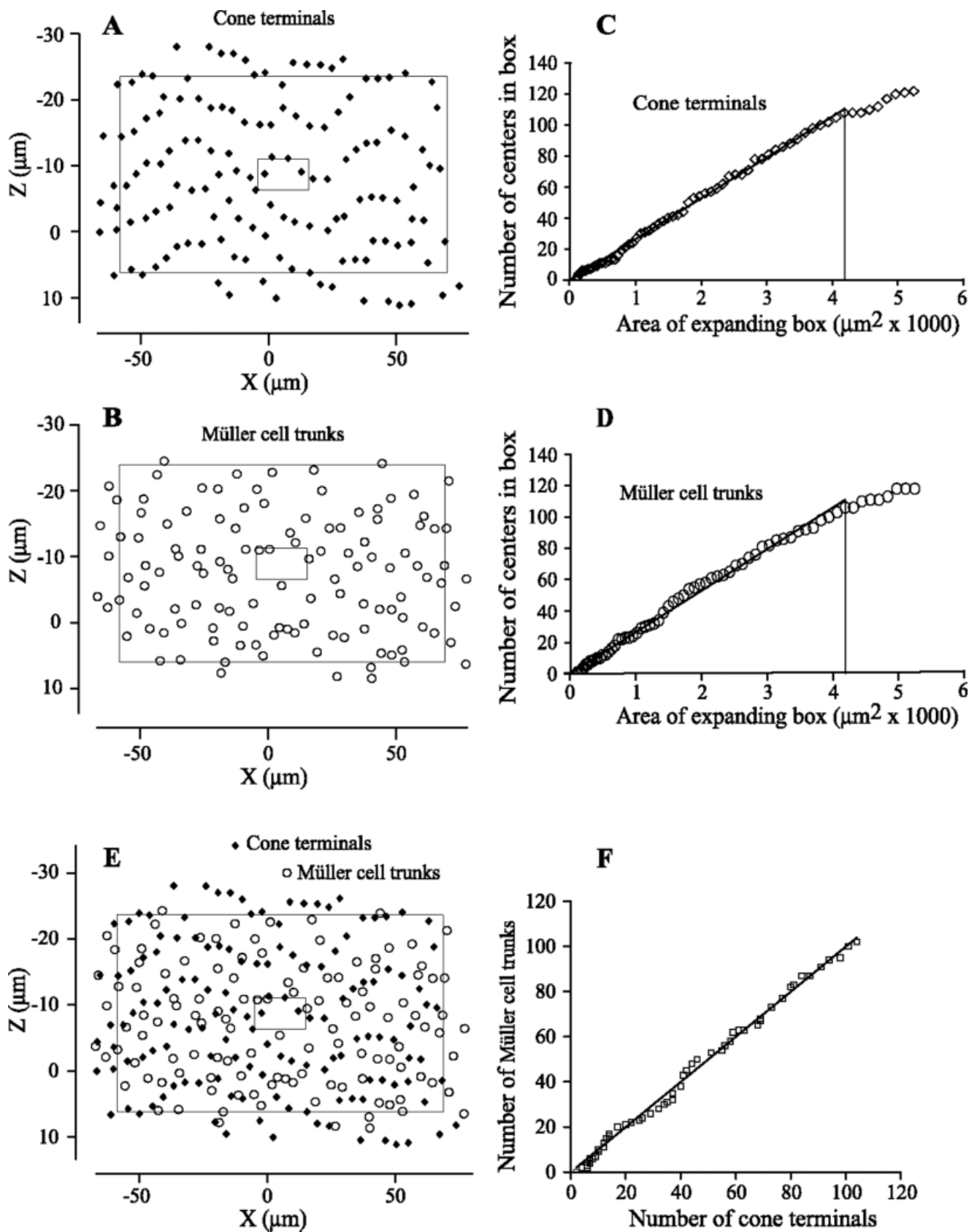


Fig. 4. Three methods of data analysis demonstrate equal numbers of cone terminals and Müller cell trunks. **A,B:** The centers of cone terminals (A) and of Müller cell trunks (B) after rotation of their raw coordinates (Fig. 2B) into the horizontal plane (see Materials and Methods section). Scales differ for X and Z coordinates. The large boxes extend 64.00 μm in the +X and -X directions from the center and 14.89 μm (0.2327 times as far) in the +Z and -Z directions. The small boxes extend 10.00 μm in the +X and -X directions and 2.0327 μm in the +Z and -Z directions. This aspect ratio (0.2327) and the center (5.370 μm , -8.700 μm) were determined from the maximum sampling area among the trunks. The larger box contains 101 cone

terminals and 100 Müller cell trunks. **C,D:** The expanding box method demonstrates equal densities of cone terminals (C) and Müller cell trunks (D). The counting box was expanded from the smaller to the larger boxes (see A and B) in 1.0000 μm steps for X and 0.2327 μm steps for Z. Slopes of the best fitting lines forced to go through the origin gave densities of 26,961 terminals/ mm^2 ($r^2 = 0.996$) and 26,959 trunks/ mm^2 ($r^2 = 0.995$). **E,F:** Number of Müller cell trunks (filled diamonds in E) equals the number of cone terminals (open circles in E) in the expanding box. The slope of the best fitting line forced to go through the origin (F) is 0.999 with an r^2 of 0.994.

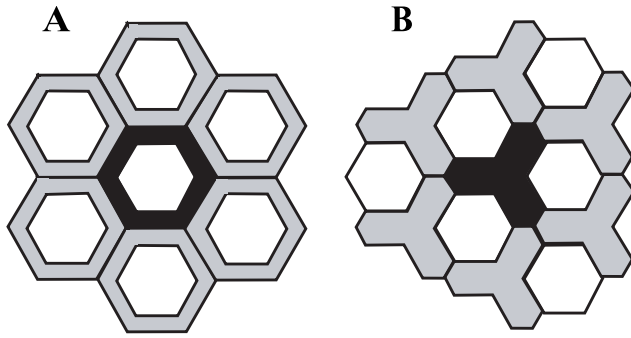


Fig. 5. Simple models for glial coating of cone terminals. Given equal numbers of Müller cell trunks (gray and black) and cone terminals (white hexagons), each trunk might be devoted exclusively to one terminal (A), or each trunk might coat a portion of several terminals (B). In A, terminals would be separated by two layers of Müller cell processes; in B, terminals would be separated by a single layer.

ways be occupied by two different Müller cells, as shown in Figure 5A. In an alternative model, shown in Figure 5B, the space between adjacent terminals would mostly be occupied by one Müller cell process. We found examples of both descriptions, with adjacent terminals separated by the processes of two Müller cells (right side of the center terminal in Fig. 3A, magnified in Fig. 3D) or by the processes of one (left side of the center terminal in Fig. 3A). Thus, neither of the models in Figure 5 correctly describes the actual arrangement.

To determine the arrangement, we reconstructed the coating around the bases of 10 terminals, composed of two groups of contiguous terminals and a single terminal. We show these coatings in the horizontal plane at the bases of the terminals (Fig. 6A–C). Each Müller cell trunk has its own color. Where a process of one trunk separates adjacent terminals, thick lines of the same color mark both terminals' perimeters. Where the processes of two trunks separate adjacent terminals, two medium lines of different colors mark the two terminals' perimeters. Finally, where we identified one Müller cell trunk coating a terminal but did not know whether there was another one between that terminal and its neighbor, we used a thin line of the color of the identified trunk to mark the one terminal's perimeter. (The thin lines are mainly at the tops and bottoms of terminals.) There is a small "hole" in the coating between terminals #46 and #60 and between #52 and its right-hand neighbor; these fenestrations allow gap junctions between adjacent terminals (Tsukamoto et al., 1992).

Measurements from these data revealed that each Müller cell coated an average of $38\% \pm 24\%$ (mean \pm SD) of a terminal's perimeter (Fig. 7A). (Inversely, a given terminal was coated by an average of 2.6 ± 0.7 Müller cells.) The processes of just one Müller cell occupied the space around an average of half (48%) of a terminal's perimeter (Fig. 7B), and the processes of two Müller cells occupied the space around the remainder (52%).

Figure 6D–F is a schematic version of the reconstructions in Figure 6A–C. In the schematics, wide, filled blocks correspond to regions between adjacent terminals occupied by one Müller cell; medium-wide, filled blocks correspond to regions occupied by two. Where the number of contributing trunks separating adjacent terminals is not

known, as indicated by the thin lines in the reconstructions, the possible second trunk is represented by an open block. Finally, black blocks represent trunks that did not coat a reconstructed terminal but nonetheless occupied space between that terminal and its adjacent terminals.

Each schematic terminal has two numbers within it. The first number indicates how many trunks coat it. The second number indicates how many trunks tile the space around it, that is, its "neighborhood". Each + associated with the second number tallies an open block around that terminal in the schematic, where there *may* be an additional trunk in the neighborhood. For example, in Figure 6C, terminal #52 is coated by two Müller cells (red and green); the schematic in the corresponding Figure 6F indicates that two more Müller cells (black) occupy the neighborhood of this terminal. The numbers in terminal #52 thus read as follows: 2 for the coatings, 4 for the Müller cells that are *definitely* in the neighborhood of the terminal, and ++ for up to two more Müller cells that *may* be in the neighborhood. Clearly, more Müller cells tile the neighborhood of a terminal than actually coat that terminal.

Assuming that half of the uncertain neighbors (+) are true neighbors, the average number of Müller cells in the neighborhood of each of the 10 cone terminals in Figure 6 is the total number of definite neighbors (41) plus half of the total number of possible neighbors ($14/2 = 7$), divided by the number of terminals: $48/10 = 4.8$. Conversely, because there are equal numbers of Müller cells and terminals, each Müller cell must be in the neighborhood of 4.8 terminals. This finding raises a caution: by light microscopy a fully stained Müller cell, although actually coating just two to three terminals, is likely to be in the neighborhood of twice as many terminals and thus appear to coat many more than two to three of them.

Clearly, equal densities do not require a simple 1:1 ensheathing as in Figure 5A or the simple tiling pattern as in Figure 5B. The actual tiling is more complex, as illustrated by the models in Figure 6G,H. The tiles in the models have the following properties that closely reflect the quantitative results: (1) Our results show that the numbers of cone terminals and Müller cells are equal. This property requires that each Müller cell coat an amount of perimeter equal to that of one whole terminal. (2) In Figure 6G, where terminals pack squarely, each Müller cell coats 2 terminals; in Figure 6H, where terminals pack triangularly, each Müller cell coats 3 terminals. In a mixture of geometries, each Müller cell would coat an average of 2.5 terminals. Our results show 2.6. (3) In turn, each terminal is coated by 2 (Fig. 6G) or 3 (Fig. 6H) Müller cells, so in a mixture of geometries, each terminal would be coated by an average of 2.5 Müller cells. (4) The space around half of a terminal's perimeter is tiled by one Müller cell, half by two. Our data indicate 48%/52%. (5) Each terminal has 4 (Fig. 6G) or 6 (Fig. 6H) Müller cells in its neighborhood, so in a mixture of geometries, an average of 5 Müller cells tile the space between terminals. Our data show 4.8.

How Müller cells partition the OPL

Müller cells partition the underlying neuropil differently from the way they partition cone terminals. Indeed,

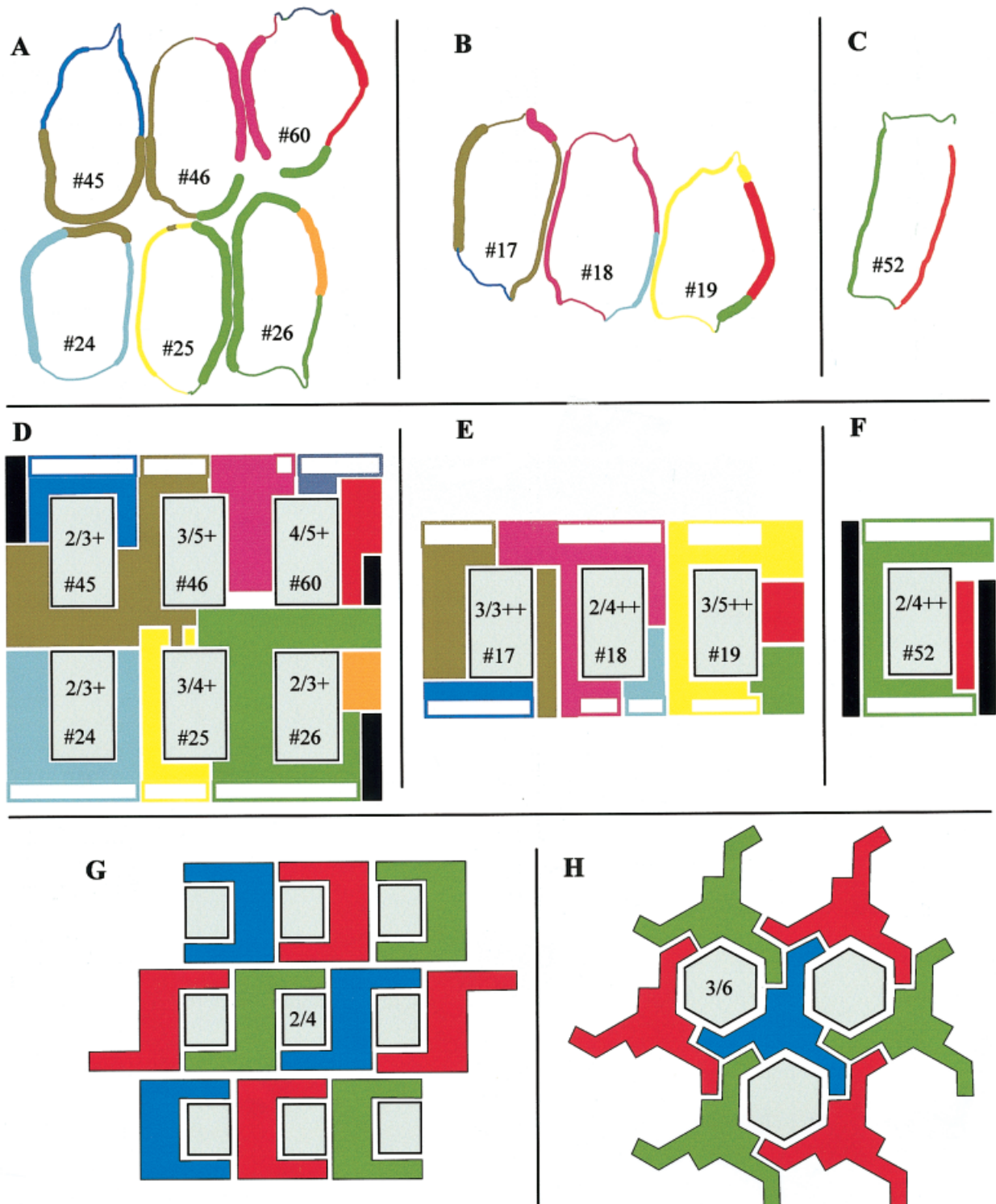


Fig. 6. Divergence of each Müller cell onto cone terminals and convergence of Müller cells onto each cone terminal, reconstructed from serial sections. **A–C:** Reconstructions of the Müller cell coatings of six, three, and one terminals whose locations are mapped in Figure 2A. The coating patterns were reconstructed at the level of the plus (+) and asterisk (*) symbols in Figure 3A and are shown here in the

horizontal plane at the bases of the terminals. See text for more details. **D–F:** Schematic versions of A–C. See text for details. **G,H:** Models of how Müller cells coat cone terminals and tile the space between them. The terminals are squarely packed in G, triangularly packed in H. The actual packing in the retina is a mixture of these geometries.

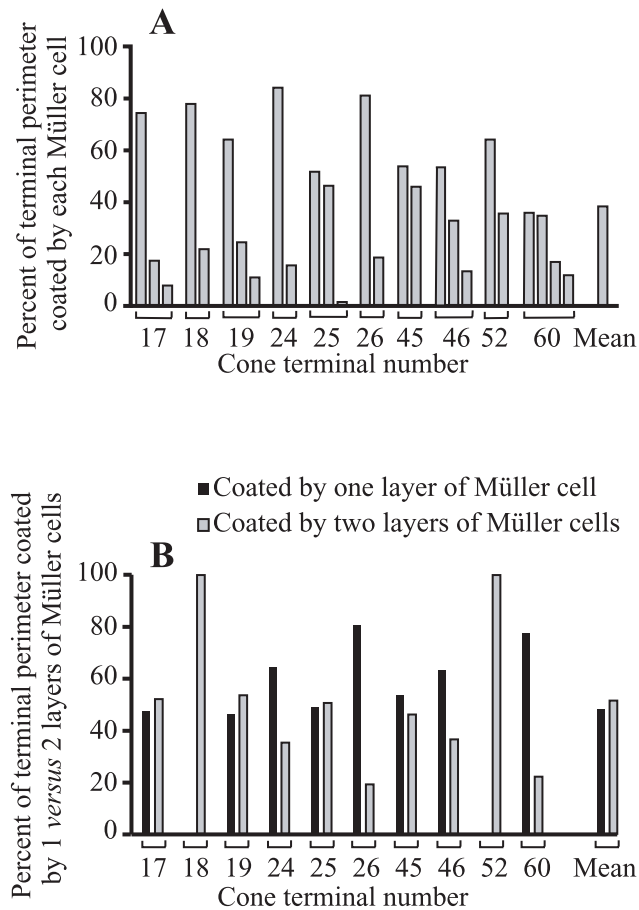


Fig. 7. Coating of cone terminals. **A:** The percentage of each cone terminal's perimeter coated by a particular Müller cell. These data were taken from the reconstructions of the cone terminals in Figure 6A–C. On average, each Müller cell coated $38.5\% \pm 24.2\%$ (mean \pm SD) of a cone terminal's perimeter, suggesting that each terminal is coated by $(1/0.385 =) 2.6 \pm 0.7$ Müller cells. **B:** The percentage of each terminal's perimeter that has one versus two Müller cells in the interstices between that terminal and its contiguous terminals. These values were also taken from the cone terminals shown in Figure 6A–C, but excluded the perimeter marked with thin lines. On average, $48\% \pm 27\%$ of the neighborhood of each terminal's perimeter is occupied by one Müller cell, and $52\% \pm 27\%$ by two.

Figure 3B,C shows that outside the region of the ascending trunk, the neuropil is continuous beneath adjacent terminals, as marked by the arrows. We reconstructed two Müller cells through the depth of the OPL (the green one in Fig. 6A coating terminals #25, #26, #46, and #60 and the cyan one in Fig. 6A coating terminal #24). As the word “trunk” suggests, the Müller process resembles a tree trunk. In the region we studied, the trunk is longer in the Z-direction, $\sim 1.5 \mu\text{m}$, than the X-direction, from $0.25 \mu\text{m}$ to $1 \mu\text{m}$. Thus, Figure 8A shows (solid) trunks in the OPL, below the space between the “footprints” of the terminals (dashed outlines). Within the OPL, below the cone terminal, the surface area of these trunks is $\sim 30 \mu\text{m}^2$.

Thus, Müller cell processes (1) ascend between “cylinders” of neuropil that underlie each terminal without substantially penetrating those cylinders, (2) completely coat the entire perimeter of the terminal's secretory face with

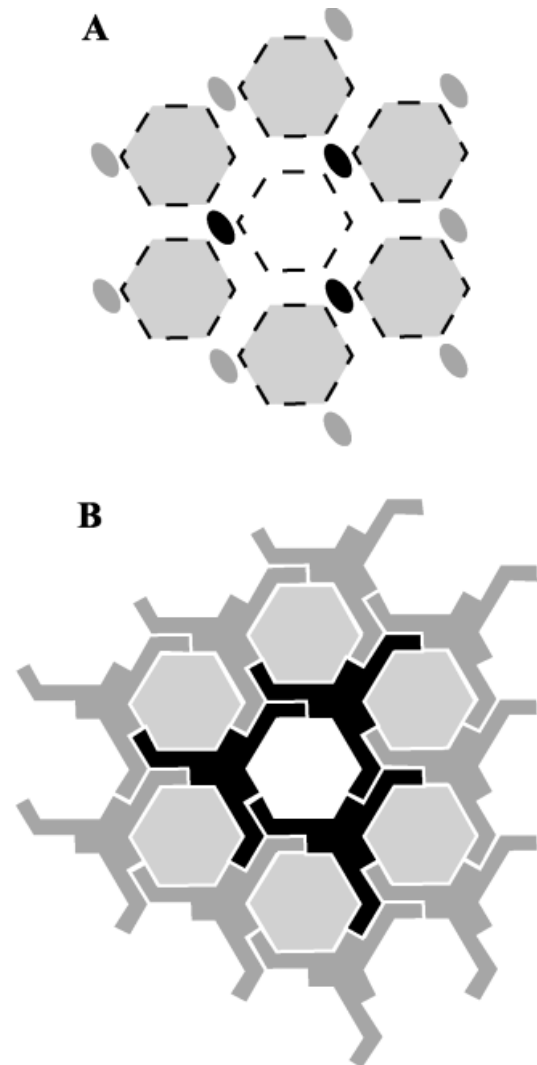


Fig. 8. The spatial relationship between Müller cells and cone terminals. **A:** In the OPL, Müller cell trunks (ovals) ascend through the neuropil below and between the projected footprints of the cone terminals (dashed hexagons). **B:** At the level of the cone terminals, six (gray) terminals surround a (white) terminal. Every gray terminal is coated by a Müller cell that also coats the white terminal. Thus, the three (black) Müller cells that remove transmitter and potassium ions released directly by the center terminal also remove these substances released by its neighbors. The three Müller cells coating each cone terminal may constitute a functional unit of transmitter uptake, providing a common environment for a cone terminal and its immediate neighbors.

at least two layers of glial membrane of one Müller cell, and (3) overlap over half of the perimeter, giving a quadruple layer of glial membrane (Fig. 8B, which is redrawn from the model in Fig. 6H to correspond with the perspective of Fig. 8A). As a result, glutamate released at the secretory face can diffuse inward into a considerable volume of neuropil (roughly $7.5 \mu\text{m} \times 5 \mu\text{m} \times \sim 5 \mu\text{m}$ deep, approximately $200 \mu\text{m}^3$) without encountering membranes of Müller cell trunks. Moreover, deep in the OPL, glutamate can diffuse laterally (arrows in Fig. 3B,C) from this volume into the deep neuropil underneath neighboring terminals.

DISCUSSION

The anatomic relationship between Müller cells and cone terminals that we find in macaque is similar to that reported in the only other case studied, the tiger salamander (Sarantis and Mobbs, 1992). Specifically, on their way from the inner nuclear layer to the photoreceptor terminals, Müller cell processes in the tiger salamander do not extend laterally into the OPL beneath each terminal and thus do not interfere with diffusion of glutamate within the OPL underneath each terminal. However, each of their two serially sectioned tiger salamander Müller cells completely surrounded at least six photoreceptors and partially coated several others, many more than what we found in the macaque fovea. The smaller number of photoreceptors coated by the Müller cells in our study may be because we studied a primate, or it may be because we studied the fovea. Finally, the tiger salamander Müller cell processes appear to fill the OPL underneath the regions where terminals abut (cf. Fig. 4 of Sarantis and Mobbs, 1992), but in the macaque, the OPL processes occupy only a small portion of that volume (ovals in Fig. 8A).

One Müller cell per cone terminal in the fovea

The present work resolves uncertainty regarding the numerical relationship of Müller cells to cone terminals in the fovea. Krebs and Krebs (1989) assumed that the arrays of cone terminals and Müller cell nuclei were both monolayers, made counts from tangential sections, and found roughly half the density of Müller cells ($17,000 \text{ mm}^{-2}$) as cone terminals ($31,000 \text{ mm}^{-2}$ to $36,000 \text{ mm}^{-2}$) in macaque fovea. Figure 1, however, shows that Müller cell nuclei reside in roughly two layers, which would double the $17,000 \text{ mm}^{-2}$ value. Indeed, Distler and Dreher (1996) found 30,000 and 37,000 Müller cells mm^{-2} in the foveae of two macaque monkeys, which led Chao et al. (1997) to speculate that in the fovea, Müller cell density could be related to cone terminal density. Here, we go further and establish, by three different methods of analysis (Fig. 4), that the fovea contains precisely equal densities of Müller cells and cone terminals.

Is there a reason that the densities of Müller cells and cone terminals are strictly equal? Equality of numbers is required for the tiling relationship between foveal Müller cells and cone terminals shown in the model in Figure 8B, and this arrangement may be important for optimal functioning of midget cell circuits in macaque fovea. Consider the midget ganglion cell whose receptive-field center is driven by the one (white) cone terminal in this figure and whose receptive-field surround is driven by the six (light gray) adjacent cone terminals. Correspondingly, the three (black) Müller cells that coat the (white) cone terminal also coat the six (light gray) adjacent terminals. The three Müller cells coating each cone terminal thus may constitute a functional unit of transmitter uptake, providing a common chemical environment for the cones responsible for a midget ganglion cell's center and surround. The fovea would be special in this regard because, in this region, midget ganglion cell centers are driven by one cone.

The situation in peripheral retina is different. Indeed, Krebs and Krebs (1987) found twice as many Müller cells ($16,000 \text{ mm}^{-2}$) as cone terminals ($8,000 \text{ mm}^{-2}$) at an eccentricity of approximately 30 degrees from the fovea,

and Distler and Dreher (1996) found a similar density of Müller cells at that eccentricity. The number of Müller cells per cone terminal thus appears to increase above one outside the fovea, where Müller cells serve numerous rod as well as cone terminals.

Müller cells and macular disease

Because Müller cells affect retinal metabolic and synaptic function, they could be a primary cause of some retinal diseases. For example, Müller cells have been implicated in juvenile X-linked retinoschisis (Yanoff et al., 1968; Deutman, 1977; Condon et al., 1986; Reid et al., 1999). In light of its 1:1 relationship to cone terminals, the macula may be particularly vulnerable to Müller cell pathology. Indeed, Müller cells have been proposed as the initiator of cystoid macular degeneration (Loeffler et al., 1992), idiopathic macular holes, and foveomacular schisis (Gass, 1999). In addition, DiLoreto et al. (1995) reported that changes in Müller cells that are normally regarded as "reactive", namely, production of glial fibrillary acidic protein, preceded degenerative changes in photoreceptors in age-related retinal degeneration in rat, raising the possibility that Müller cell disease may underlie some forms of age-related macular degeneration in humans.

The geometric relationship between Müller cells and foveal cone terminals suggests that death of one (blue) Müller cell (in Fig. 6H) could partially denude the three (white) cone terminals that it served and greatly expand those terminals' immediate extracellular space. Without a narrow synaptic cleft, vesicular release might not cause the large peaks in glutamate concentration needed by autoreceptors or glutamate transporters on the cone terminal to control release (Picaud et al., 1995; Scanziani et al., 1997; Min et al., 1998; Roska et al., 1998; Koulen et al., 1999). The absence of this negative feedback mechanism might increase the tonic release rate, leading to exhaustion of the synaptic terminal and perhaps death of the white cones. Conceivably, loss of the one (blue) Müller cell and the three (white) cones would create large extracellular spaces for the six surrounding (red and green) Müller cells, causing their death, the death of their surrounding cones, and so on. This mechanism is obviously highly speculative, but it suggests a novel approach to thinking about macular disease.

Müller cell framework permits transmitter diffusion to many receptor sites

The glial cell framework for cone terminals differs strikingly from that of other central synapses. For example, Bergman glia completely coat all synapses on Purkinje cell spines, thus segregating every active zone from its neighbors (Lehre and Danbolt, 1998). By contrast, astrocytes in CA1 of hippocampus coat approximately half of the axospinous synapses, with coatings that are often incomplete (Ventura and Harris, 1999). These glial frameworks are of fine mesh, and glutamate can diffuse within a two-dimensional cleft for at most 100 nm before encountering glial membrane and their associated transporters. Spillover of glutamate from one synapse to a neighboring one may occur, particularly where astrocytes fail to separate two active zones and because synapses wrapped in the same glial package will experience more mutual spillover than those separated by glial membranes (Lehre and Danbolt, 1998; Rusakov and Kullmann, 1998). During intense release, transmitter may even spill over to affect

low affinity receptors at adjacent synapses (Luján et al., 1997; Kullmann and Asztely, 1998; Rusakov et al., 1999). However, this spillover is confined to two dimensions and small spatial scale (Danbolt, 2001).

For giant central synapses, such as the calyceal synapse in the auditory brainstem, multiple active zones are unseparated by glial fingers (Otis et al., 1996). The calyx appears to be topologically one-dimensional, because each active zone directly abuts a postsynaptic process across a 20-nm cleft. However, spillover can occur on a larger scale into the second dimension. In the glomerular synapse in the thalamus, a spheroidal cluster of glutamatergic and GABAergic processes are wrapped in a sheet of astrocytes (Majorossy et al., 1965; Peters and Palay, 1966; Guillery, 1969); each active zone abuts a postsynaptic process, forming an inherently one-dimensional synapse. However, transmitter also spills into the higher dimensional extracellular space of the cluster before reaching the astrocytic shell. In these examples, primary transmission occurs on the scale of 20 nm.

By contrast, as can be appreciated in the photomicrographs in Figure 3, the Müller cell framework permits diffusion of glutamate from its (~20) release sites associated with synaptic ribbons on the secretory face of one cone terminal to the large number (~500) of receptor clusters on dendrites associated with a terminal (Chun et al., 1996). The secretory face of a foveal cone terminal has an area of ~50 μm^2 , giving a domain of ~2.5 μm^2 per release site. If this domain were configured as an area 0.8 μm high by 3 μm wide, no receptor cluster would be more than 1,500 nm from a release site alongside a synaptic ribbon (Schein et al., 1996).

In more detail, these receptor clusters are distributed over a broad scale of distance and dimension (Schein et al., 1996; Vardi et al., 1998, 2000; Morigiwa and Vardi, 1999; Haverkamp et al., 2000, 2001): A pulse of glutamate released at the active zone encounters in one dimension, 10 nm away, iGluR receptor clusters directly across the synaptic cleft (on horizontal cell spines). It encounters along the two-dimensional surface of the terminal, ~600 nm away, mGluR6 receptors near the mouth of the invagination (on the invaginating dendrites of inner midget and diffuse bipolar cells), ~1,000 nm away, iGluR receptors on triad-associated contacts (on OFF midget bipolar cell dendrites), and ~1,500 nm away, iGluR and mGluR6 receptors on basal contacts (on outer and inner diffuse bipolar cell dendrites, respectively). In three dimensions, it encounters iGluR receptors (on horizontal cell dendrites) 1,500–1,800 nm away. Glutamate should be able to diffuse these distances in a time scale on the order of a millisecond (Sarantis et al., 1993; Clements, 1996; Ribble et al., 1997; Overstreet et al., 1999). That a pulse of transmitter could diffuse 1,000 nm or more to cause an excitatory postsynaptic current may seem surprising, but recent electrophysiological recordings from bipolar-cone pairs provide ample confirmation (DeVries and Schwartz, 1999; DeVries, 2000).

Indeed, glutamate could even diffuse from the center of the secretory face of the cone terminal laterally along the secretory face to receptors at the perimeter of the terminal and Müller cell membrane, a distance of 2–3 μm , in less than 10 msec. Glutamate transporters on Müller cell processes (see below) bind glutamate quickly in this time frame (Bergles and Jahr, 1998). Therefore, for this diffusion to occur, it is critical that Müller glial processes are

absent from the neuropil immediately underlying the cone terminals, which is exactly what we show here.

Just beneath the terminal's secretory face, glutamate reaching the edge of the terminal encounters multilayered Müller cell wrappings that should reduce lateral spillover between terminals (Fig. 8B), but not necessarily to zero (S. DeVries, personal communication). Müller cell membranes at this site thus help preserve independent activity between the midget bipolar cells that provide the private pathways for each foveal cone and are responsible for visual resolution in macaque fovea as fine as the dense array of foveal cones.

Glutamate diffusing more deeply into the neuropil encounters Müller membrane only at the trunks (Fig. 8A, ovals), so lateral spillover deep in the OPL (arrows in Fig. 3B,C) to receptor clusters on horizontal cells underneath neighboring terminals may proceed unimpeded. Unlike glutamate receptors on midget bipolar cells, those on horizontal cells are presumably designed to respond to glutamate from a larger distance, that is, to slower and lower concentration pulses. Because horizontal cells already sum responses over large numbers of cone terminals, this inter-terminal spillover is not disadvantageous.

Does the glial framework's transport capacity match the estimated flux of glutamate?

The Müller cell removes neuroactive substances (e.g., potassium, GABA, and glutamate) released into the extracellular space by synaptic activity (Newman et al., 1984; Ripps and Witkovsky, 1985; Newman and Reichenbach, 1996). Scavenging should be vigorous to prevent disasters like spreading depression and neurotoxicity but should also be precisely tuned to optimize the spatiotemporal concentration of each substance. Although neurons, including cone terminals and bipolar dendrites (Massey et al., 1997; Vandenbranden et al., 2000), also express transporters, the following speculative discussion follows findings that Müller glia dominate glutamate transport in the retina (Kennedy et al., 1974; White and Neal, 1976; Ehinger, 1977; Lehre et al., 1997; Bergles and Jahr, 1998), as glial cells probably do elsewhere as well (Lehre and Danbolt, 1998; Rusakov and Kullmann, 1998; Pow et al., 2000).

The band of Müller cell membrane that coats the perimeter of a cone terminal, ~25 μm in length (Fig. 8B), rises 2 μm from the base of the terminal with 1.5-fold lapping, to present a membrane surface area of ~75 μm^2 of Müller cell per cone terminal. Beneath the terminal, within the OPL, the Müller cell trunk has a surface area of ~30 μm^2 (ovals in Fig. 8A). Although the density and distribution of EAAT1 transporters on Müller cell membrane has not been determined, here we assume a density of 5,000 EAAT1 μm^{-2} (Derouiche and Rauen, 1995; Rauen et al., 1996; Lehre and Danbolt, 1998). In that case, these two Müller cell surface areas could represent 375,000 and 150,000 EAAT1 molecules per cone terminal. Müller cells contain three additional excitatory amino acid transporters (Eliasof et al., 1998a,b), and as noted above, the neurons contain transporters as well, so these numbers of EAAT1 molecules may underestimate the total number of glutamate transporters.

Glutamate transporters require ~100 msec for transport (Wadiche et al., 1995; Otis and Jahr, 1998; Wadiche and Kavanaugh, 1998). The precise number of glutamate

molecules in a synaptic vesicle is not known, with estimates ranging from 400 to 4,000 (Danbolt, 2001). Assuming a glutamate concentration of 100 mM (Danbolt, 2001), the synaptic vesicles in our material, with an inner diameter of 35 nm, would have 1,500 molecules, in the middle of this range. Assuming a release rate of $\sim 1,000$ quanta sec^{-1} , from ~ 20 active zones each releasing at 50 quanta sec^{-1} (Ashmore and Copenhagen, 1983; Rieke and Schwartz, 1996; Rao-Mirotnik et al., 1998), we estimate that each cone terminal releases $\sim 1.5 \times 10^6$ glutamate sec^{-1} , or $\sim 150,000$ glutamate molecules over the 100-msec transport time. Thus, despite the impressive tonic flux, the Müller cell framework by itself, with perhaps $\sim 500,000$ glial EAAT1 transporters per cone terminal, seems to create an adequate sink for glutamate, in these estimations several times as much as needed.

ACKNOWLEDGMENTS

We thank Steve Herr for valuable guidance in tracking Müller cells. We thank Dr. Yoshihiko Tsukamoto, Patricia Masarachia, and Sally Shrom for preparing the EM material. We also thank Kazuki Uema and Lisa Travis for printing. Portions of this work were previously presented in abstract form in Klug et al. (1991) and in Burris et al. (1999).

LITERATURE CITED

- Ashmore JF, Copenhagen DR. 1983. An analysis of transmission from cones to hyperpolarizing bipolar cells in the retina of the turtle. *J Physiol (Lond)* 340:569–597.
- Bergles DE, Jahr CE. 1998. Glial contribution to glutamate uptake at Schaffer collateral-commissural synapses in the hippocampus. *J Neurosci* 18:7709–7716.
- Bergles DE, Diamond JS, Jahr CE. 1999. Clearance of glutamate inside the synapse and beyond. *Curr Opin Neurobiol* 9:293–298.
- Burris CJ, Sterling P, Schein S. 1999. One Müller cell per foveal cone in macaque monkey. *Invest Ophthalmol Vis Sci Suppl* 40:S238.
- Chao TL, Grosche J, Friedrich KJ, Biedermann B, Francke M, Pannicke T, Reichelt W, Wulst M, Muhle C, Pritz-Hohmeier S, Kuhrt H, Faude F, Drommer W, Kasper M, Buse E, Reichenbach A. 1997. Comparative studies on mammalian Müller (retinal glial) cells. *J Neurocytol* 26:439–454.
- Chun M-H, Grünert U, Martin PR, Wässle H. 1996. The synaptic complex of cones in the fovea and in the periphery of the macaque monkey retina. *Vision Res* 36:3383–3395.
- Clements JD. 1996. Transmitter time course in the synaptic cleft: its role in central synaptic function. *Trends Neurosci* 19:163–171.
- Condon GP, Brownstein S, Wang NS, Kearns AF, Ewing CC. 1986. Congenital hereditary (juvenile X-linked) retinoschisis: histopathologic and ultrastructural findings in three eyes. *Arch Ophthalmol* 104:576–583.
- Danbolt NC. 2001. Glutamate uptake. *Prog Neurobiol* 65:1–105.
- Derouiche A, Rauen T. 1995. Coincidence of L-glutamate:L-aspartate transporter (GLAST) and glutamine synthetase (GS) immunoreactions in retinal glia: evidence for coupling of GLAST and GS in transmitter clearance. *J Neurosci Res* 42:131–143.
- Deutman AF. 1977. Vitreoretinal dystrophies. In: Krill A, Archer DB, editors. Hereditary retinal and choroidal diseases. Vol. 2. New York: Harper & Row. p 1043–1108.
- DeVries SH. 2000. Bipolar cells use kainate and AMPA receptors to filter visual information into separate channels. *Neuron* 28:847–856.
- DeVries SH, Schwartz EA. 1999. Kainate receptors mediate synaptic transmission between cones and “Off” bipolar cells in a mammalian retina. *Nature* 397:157–160.
- DiLoreto DA Jr, Martzen MR, del Cerro C, Coleman PD, del Cerro M. 1995. Müller cell changes precede photoreceptor cell degeneration in the age-related retinal degeneration of the Fischer 344 rat. *Brain Res* 198:1–14.
- Distler C, Dreher Z. 1996. Glia cells of the monkey retina. II. Müller cells. *Vision Res* 36:2381–2394.
- Dogiel AS. 1893. Neuroglia der Retina des Menschen. *Arch Mikrosk Anat* 41:612–623.
- Dreher Z, Robinson SR, Distler C. 1992. Müller cells in vascular and avascular retinæ: a survey of seven mammals. *J Comp Neurol* 323:59–80.
- Ehinger B. 1977. Glial and neuronal uptake of GABA, glutamic acid, glutamine and glutathione in the rabbit retina. *Exp Eye Res* 25:221–234.
- Eliasof S, Arriza JL, Leighton BH, Amara SG, Kavanaugh MP. 1998a. Localization and function of five glutamate transporters cloned from the salamander retina. *Vision Res* 38:1443–1454.
- Eliasof S, Arriza JL, Leighton BH, Kavanaugh MP, Amara SG. 1998b. Excitatory amino acid transporters of the salamander retina: identification, localization, and function. *J Neurosci* 18:698–712.
- Gass JD. 1999. Müller cell cone, an overlooked part of the anatomy of the fovea centralis: hypotheses concerning its role in the pathogenesis of macular hole and foveomacular retinoschisis. *Arch Ophthalmol* 117:821–823.
- Guillery RW. 1969. The organization of synaptic interconnections in the laminae of the dorsal lateral geniculate nucleus of the cat. *Z Zellforsch Mikrosk Anat* 96:1–38.
- Haverkamp S, Grünert U, Wässle H. 2000. The cone pedicle, a complex synapse in the retina. *Neuron* 27:85–95.
- Haverkamp S, Grünert U, Wässle H. 2001. The synaptic architecture of AMPA receptors at the cone pedicle of the primate retina. *J Neurosci* 21:2488–2500.
- Herr SS, Klug K, Sterling P, Schein SJ. 1997. OFF midget bipolar dendrites have similar densities at their distal tips and more proximally. *Invest Ophthalmol Vis Sci Suppl* 38:S618.
- Kennedy AJ, Voaden MJ, Marshall J. 1974. Glutamate metabolism in the frog retina. *Nature* 25:50–52.
- Klug K, Schein SJ, Masarachia P, Sterling P, Tsukamoto, Y. 1991. Identification of all cells in a small patch of fovea of macaque retina. *Soc Neurosci Abstr* 17:1375.
- Koulen P, Kuhn R, Wässle H, Brandstätter JH. 1999. Modulation of the intracellular calcium concentration in photoreceptor terminals by a presynaptic metabotropic glutamate receptor. *Proc Natl Acad Sci U S A* 96:9909–9914.
- Krebs W, Krebs IP. 1987. Quantitative morphology of the primate peripheral retina (*Macaca irus*). *Am J Anat* 179:198–208.
- Krebs W, Krebs IP. 1989. Quantitative morphology of the central fovea in the primate retina. *Am J Anat* 184:225–236.
- Kullmann DM, Asztely F. 1998. Extrasynaptic glutamate spillover in the hippocampus: evidence and implications. *Trends Neurosci* 21:8–14.
- Lehre KP, Danbolt NC. 1998. The number of glutamate transporter subtype molecules at glutamatergic synapses: chemical and stereological quantification in young adult rat brain. *J Neurosci* 18:8751–8757.
- Lehre KP, Davanger S, Danbolt NC. 1997. Localization of the glutamate transporter protein GLAST in rat retina. *Brain Res* 744:129–137.
- Loeffler KU, Li ZL, Fishman GA, Tso MO. 1992. Dominantly inherited cystoid macular edema. A histopathologic study. *Ophthalmology* 99:1385–1392.
- Luján R, Roberts JD, Shigemoto R, Ohishi H, Somogyi P. 1997. Differential plasma membrane distribution of metabotropic glutamate receptors mGluR1 alpha, mGluR2 and mGluR5, relative to neurotransmitter release sites. *J Chem Neuroanat* 13:219–241.
- Majorossy K, Réthelyi M, Szentágothai J. 1965. The large glomerular synapse of the pulvinar. *J Hirnforsch* 7:415–432.
- Massey SL, Koomen JM, Liu S, Lehre KP, Danbolt NC. 1997. Distribution of the glutamate transporter GLT-1 in the rabbit retina. *Invest Ophthalmol Vis Sci Suppl* 38:S689.
- Min M-Y, Rusakov DA, Kullmann DM. 1998. Activation of AMPA, kainate, and metabotropic receptors at hippocampal mossy fiber synapses: role of glutamate diffusion. *Neuron* 21:561–570.
- Morigiwa K, Vardi N. 1999. Differential expression of ionotropic glutamate receptor subunits in the outer retina. *J Comp Neurol* 405:173–184.
- Müller H. 1851. Zur Histologie der Netzhaut. *Z Wiss Zool* 3:234–237.
- Newman E, Reichenbach A. 1996. The Müller cell: a functional element of the retina. *Trends Neurosci* 19:307–312.
- Newman EA, Frambach DA, Odette LL. 1984. Control of extracellular potassium levels by retinal glial cell K⁺ siphoning. *Science* 225:1174–1175.

- Otis TS, Jahr CE. 1998. Anion currents and predicted glutamate flux through a neuronal glutamate transporter. *J Neurosci* 18:7099–7110.
- Otis TS, Wu YC, Trussell LO. 1996. Delayed clearance of transmitter and the role of glutamate transporters at synapses with multiple release sites. *J Neurosci* 16:1634–1644.
- Overstreet LS, Kinney GA, Liu YB, Billups D, Slater NT. 1999. Glutamate transporters contribute to the time course of synaptic transmission in cerebellar granule cells. *J Neurosci* 19:9663–9673.
- Peters A, Palay SL. 1966. The morphology of laminae A and A1 of the dorsal nucleus of the lateral geniculate body of the cat. *J Anat* 100:451–486.
- Picaud S, Larsson HP, Wellis DP, Lecar H, Werblin F. 1995. Cone photoreceptors respond to their own glutamate release in the tiger salamander. *Proc Natl Acad Sci U S A* 92:9417–9421.
- Polyak S. 1941. *The retina*. Chicago: The University of Chicago Press.
- Pow DV, Barnett NL, Penfold P. 2000. Are neuronal transporters relevant in retinal glutamate homeostasis? *Neurochem Int* 37:191–198.
- Rao-Mirotnik R, Buchsbaum G, Sterling P. 1998. Transmitter concentration at a three-dimensional synapse. *J Neurophysiol* 80:3163–3172.
- Ramón y Cajal, S. 1892. *The structure of the retina*. English translation (1972). Springfield, IL: Charles C Thomas.
- Rauen T, Rothstein JD, Wässle H. 1996. Differential expression of three glutamate transporter subtypes in the rat retina. *Cell Tissue Res* 286:325–336.
- Reichenbach A, Fromter C, Engelmann R, Wolburg H, Kasper M, Schnitzer J. 1995. Müller glial cells of the tree shrew retina. *J Comp Neurol* 360:257–270.
- Reid SN, Akhmedov NB, Piriev NI, Kozak CA, Danciger M, Farber DB. 1999. The mouse X-linked juvenile retinoschisis cDNA: expression in photoreceptors. *Gene* 227:257–266.
- Ribble J, Klug K, Sterling P, Schein SJ. 1997. The cleft system associated with a foveal cone terminal in Macaque. *Invest Ophthalmol Vis Sci Suppl* 38:S723.
- Rieke F, Schwartz EA. 1996. Asynchronous transmitter release: control of exocytosis and endocytosis at the salamander rod synapse. *J Physiol (Lond)* 493:1–8.
- Ripps H, Witkovsky P. 1985. Neuron-glia interaction in the brain and retina. *Prog Retinal Res* 4:181–219.
- Robinson SR, Dreher Z. 1990. Müller cells in adult rabbit retinae: morphology, distribution and implications for function and development. *J Comp Neurol* 292:178–192.
- Roska B, Gaal L, Werblin FS. 1998. Voltage-dependent uptake is a major determinant of glutamate concentration at the cone synapse: an analytical study. *J Neurophysiol* 80:1951–1960.
- Rusakov DA, Kullmann DM. 1998. Extrasynaptic glutamate diffusion in the hippocampus: ultrastructural constraints, uptake, and receptor activation. *Neuroscience* 18:3158–3170.
- Rusakov DA, Kullmann DM, Stewart MG. 1999. Hippocampal synapses: do they talk to their neighbours? *Trends Neurosci* 22:382–388.
- Sarantis M, Mobbs P. 1992. The spatial relationship between Müller cell processes and the photoreceptor output synapse. *Brain Res* 584:299–304.
- Sarantis M, Ballerini L, Miller B, Silver RA, Edwards M, Attwell D. 1993. Glutamate uptake from the synaptic cleft does not shape the decay of the non-NMDA component of the synaptic current. *Neuron* 11:541–549.
- Scanziani M, Salin PA, Vogt KE, Malenka RC, Nicoll RA. 1997. Use-dependent increases in glutamate concentration activate presynaptic metabotropic glutamate receptors. *Nature* 385:630–634.
- Schein SJ. 1988. Anatomy of macaque fovea and spatial densities of neurons in foveal representation. *J Comp Neurol* 269:479–505.
- Schein SJ, Gayed JM, Herr SS, Sterling P, Klug K. 1996. Cone ribbon synapses might supply basal synapses with glutamate. *Invest Ophthalmol Vis Sci Suppl* 37:S6.
- Smith RG. 1987. Montage: a system for three-dimensional reconstruction by personal computer. *J Neurosci Methods* 21:55–69.
- Spacek J. 1985. Relationships between synaptic junctions, puncta adherentia and the spine apparatus at neocortical axo-spinous synapses. A serial section study. *Anat Embryol (Berl)* 173:129–135.
- Tsukamoto Y, Masarachia P, Schein SJ, Sterling P. 1992. Gap junctions between the pedicles of macaque foveal cones. *Vision Res* 32:1809–1815.
- Vardi N, Morigiwa K, Wang TL, Shi YJ, Sterling P. 1998. Neurochemistry of the mammalian cone “synaptic complex”. *Vision Res* 38:1359–1369.
- Vardi N, Duvoisin R, Wu G, Sterling P. 2000. Localization of mGluR6 to dendrites of ON bipolar cells in primate retina. *J Comp Neurol* 423:402–412.
- Ventura R, Harris KM. 1999. Three-dimensional relationships between hippocampal synapses and astrocytes. *J Neurosci* 19:6897–6906.
- Vandenbranden CA, Yazulla S, Studholme KM, Kamphuis W, Kamermans M. 2000. Immunocytochemical localization of the glutamate transporter GLT-1 in goldfish (*Carassius auratus*) retina. *J Comp Neurol* 423:440–451.
- Wadiche JI, Kavanaugh MP. 1998. Macroscopic and microscopic properties of a cloned glutamate transporter/chloride channel. *J Neurosci* 18:7650–7661.
- Wadiche JI, Arriza JL, Amara SG, Kavanaugh MP. 1995. Kinetics of a human glutamate transporter. *Neuron* 14:1019–1027.
- White RD, Neal MJ. 1976. The uptake of L-glutamate by the retina. *Brain Res* 111:79–93.
- Yanoff N, Rahn EK, Zimmerman LE. 1968. Histopathology of juvenile retinoschisis. *Arch Ophthalmol* 79:49–53.